LRP 696/01 May 2001

Effect of Toroidal Current and Profile on Ballooning Instability Mechanisms in a Quasiaxisymmetric Stellarator

W.A. Cooper, S. Okamura
& K. Yamazaki

Accepted for publication in

PLASMA PHYSICS AND
CONTROLLED FUSION

ISSN 0458-5895

EFFECT OF TOROIDAL CURRENT AND PROFILE ON BALLOONING INSTABILITY MECHANISMS IN A QUASIAXISYMMETRIC STELLARATOR

W. A. COOPER
Centre de Recherches en Physique des Plasmas, Association Euratom-Confédération Suisse, Ecole Polytechnique Fédérale de Lausanne, CRPP-PPB, CH-1015 Lausanne, Switzerland

S. OKAMURA and K. YAMAZAKI
National Institute for Fusion Science, 322-6 Oroshi-cho, Toki-shi 509-5292, Japan

Abstract

Finite toroidal plasma current reduces the magnitude of the normal magnetic field line curvature near midvolume in a quasiaxisymmetric stellarator. This improves the ideal ballooning stability conditions. Near the edge of the plasma, a hollow toroidal current profile deteriorates the ballooning stability properties by enhancing the normal curvature while a parabolic current profile improves this stability because the normal curvature decreases. The magnetic field line bending term can also impact the stability properties when the normal curvatures are comparable. The local magnetic shear and the geodesic curvature vanish where the normal curvature is most destabilising. The quasiperiodic ballooning curvature contribution, unlike the normal curvature, fails to constitute a useful indicator about the localisation of ballooning structures.

1 INTRODUCTION

Quasiaxisymmetric stellarators are three-dimensional (3D) magnetic plasma confinement systen in which the magnetic field strength in Boozer magnetic coordinates [1] depends dominantly on the radial coordinate and the poloidal angle, namely $B = B(s, \theta)$ [2,3]. Designs are currently under consideration at the National Institute for Fusion Science [4] and at the Princeton Plasma Physics Laboratory [5]. Unlike configurations like Wendelstein WVII-X, quasiaxisymmetric stellarators can have a substantial bootstrap current that can modify the rotational transform significantly [2]. Furthermore, the application of unbalanced neutral beam injection can also cause a finite plasma current that can be concentrated near the magnetic axis if the energetic neutral particles reach the centre of the plasma.

Even though the bootstrap current and the neutral beam currents can destabilise external kink modes, ballooning instabilities driven by the interaction of the pressure gradient with the magnetic field line curvature can in many circumstances impose the limiting β values that can be achieved in a device. This is particularly the case in quasiaxisymmetric stellarators where the modulation of the normal curvature aligns regions where this quantity is most destabilising with those in which

the local magnetic shear vanishes as will be shown further along in this paper.

The main contribution of this article is to elucidate the impact of toroidal plasma current driven either by the bootstrap effect or by neutral beams on the mechanisms that govern the destabilisation of ballooning modes. The magnitudes and profiles of the currents prescribed do not match selfconsistent calculations from either the deposition of neutral beams or bootstrap current analysis. As there remains some controversy at present about the magnitude and profile of the current that can be achieved dependent on the model applied, the computations undertaken in this paper should be considered as scoping studies that intend to reveal the relevant physical properties rather than a detailed simulation that predicts the performance of a particular device.

The relevant physical expressions associated with the stabilisation and destabilisation of ballooning modes are presented in Sec. 2. The numerical results are described in Sec. 3 followed by conclusions and discussions in Sec. 4.

2 RELEVANT PHYSICAL EXPRESSIONS

The ideal ballooning mode equation can be succinctly expressed as [6-8]

$$\partial_\theta k_\perp^2 \partial_\theta \chi + (1-\lambda)[\kappa_p + \kappa_g(\theta - \theta_k)] = 0, \tag{1}$$

where $k_\perp^2$ represents the magnetic field line bending term that balances the driving terms represented by the quasiperiodic ballooning curvature contribution κ_p and the geodesic curvature κ_g. The eigenvalue is denoted by λ, χ corresponds to the eigenstructure, θ is the poloidal angle and θ_k is the radial wave number. The magnetic field line bending term in Boozer magnetic coordinates can be written as

$$\begin{aligned} k_\perp^2 &= \left[\frac{g_{ss}}{\sqrt{g}} - \frac{B_s^2}{\sqrt{g}B^2}\right] - 2\frac{q'(s)\Psi'(s)h_s}{\sqrt{g}B^2}|\nabla s|^2(\theta-\theta_k) \\ &+ \frac{[q'(s)\Psi'(s)]^2}{\sqrt{g}B^2}|\nabla s|^2(\theta-\theta_k)^2. \end{aligned}$$

Numerical errors in the equilibrium determination, reconstruction and in the mapping to Boozer coordinates can cause this form to become non-negative definite (for negative Jacobian $\sqrt{g}$) under some circumstances. This can be considered a useful diagnostic about the accuracy of the equilibrium state being investigated. In this equation, $0 \leq s \leq 1$ is the radial variable, g_{ss} and $|\nabla s|^2$ constitute metric elements, B_s is the radial component of the magnetic field in the covariant representation, $q(s) = \Phi'(s)/\psi'(s)$ is the inverse rotational transform, B is the magnetic field strength, $2\pi\Phi(s)$ is the toroidal magnetic flux, $2\pi\psi(s)$ is the poloidal magnetic

flux and prime ($'$) indicates the derivative of a flux surface quantity with respect to s. Furthermore, the function h_s represents the integrated local magnetic shear

$$h_s = \frac{\sqrt{g}B^2}{\Phi'(s)|\nabla s|^2}\left[\frac{g_{s\theta}}{\sqrt{g}} - \frac{J(s)B_s}{B^2}\right],$$

where $g_{s\theta}$ is another metric element and $2\pi J(s)$ is the toroidal current flux. The local magnetic shear is expressed as

$$\sqrt{g}S = \Psi'(s)\Phi''(s) - \Phi'(s)\Psi''(s) - \sqrt{g}\boldsymbol{B}\cdot\nabla h_s.$$

It is useful to note that h_s is the radial component of the field line bending vector $\boldsymbol{h} = \boldsymbol{B}\times\nabla s/|\nabla s|^2$ which is related to the local magnetic shear through the equation $S = -\boldsymbol{h}\cdot\nabla\times\boldsymbol{h}$ [9-12]. The quasiperiodic component of the ballooning curvature can be written as

$$\begin{aligned}\kappa_p &= \frac{p'(s)}{[\Psi'(s)]^2}\left[\sqrt{g}\boldsymbol{B}\cdot\nabla\left(\frac{B_s}{B^2}\right) - \frac{\partial\sqrt{g}}{\partial s}\right.\\ &+ \left.\frac{\sqrt{g}p'(s) + J(s)\Psi''(s) - I(s)\Phi''(s)}{B^2}\right],\end{aligned}$$

which is closely related to the interaction of the pressure gradient with the normal magnetic field line curvature, namely,

$$\begin{aligned}2p'(s)\sqrt{g}\boldsymbol{\kappa}\cdot\nabla s &= p'(s)|\nabla s|^2\left[\sqrt{g}\boldsymbol{B}\cdot\nabla\left(\frac{B_s}{B^2}\right) - \frac{\partial\sqrt{g}}{\partial s}\right.\\ &+ \frac{\sqrt{g}p'(s) + J(s)\Psi''(s) - I(s)\Phi''(s)}{B^2}\\ &+ \left.\frac{h_s\boldsymbol{B}\times\nabla\boldsymbol{s}\cdot\nabla\sqrt{g}}{B^2}\right].\end{aligned}$$

They differ through the modulation by the factor $|\nabla s|^2$ and by a term related to the integrated local shear. These differences are sufficient that the structure of κ_p becomes quite disimilar to that of $2p'(s)\sqrt{g}\boldsymbol{\kappa}\cdot\nabla s$. In these expressions, $2\pi I(s)$ is the poloidal current flux. For completeness, the geodesic curvature is

$$\begin{aligned}\kappa_g &= -\frac{q'(s)}{\Psi'(s)}\sqrt{g}\boldsymbol{B}\cdot\nabla\left(\frac{\boldsymbol{j}\cdot\boldsymbol{B}}{B^2}\right)\\ &= -\frac{p'(s)q'(s)}{\sqrt{g}B^2\Psi'(s)}\left[I(s)\frac{\partial\sqrt{g}}{\partial\theta} + J(s)\frac{\partial\sqrt{g}}{\partial\phi}\right].\end{aligned}$$

3 NUMERICAL RESULTS

We examine a quasiaxisymmteric stellarator configuration with 2 field periods at $\beta^* \simeq 3\%$. β^* is the root mean square value of β and is considered a more relevant measure of performance in terms of fusion power production. Magnetohydrodynamic (MHD) equilibria are computed with the fixed boundary version of the VMEC code [13]. The pressure profile prescribed is illustrated in Fig. 1a. To analyse the impact of the toroidal plasma current, we concentrate on three cases: a zero net torodal current case and cases with hollow and parabolic toroidal plasma current profile respectively given by

$$\begin{aligned} 2\pi J'(s) &= 2\pi J(1)[0.9(1-s) + 20s^3(1-s)]/1.45, \\ 2\pi J'(s) &= 4\pi J(1)(1-s). \end{aligned}$$

These profiles are displayed in Fig. 1b. For finite current, a normalised toroidal current $2\pi J_N = J(1)R_{10}/\Phi(1) = 0.2552$ is chosen, where R_{10} is the $m/n = 1/0$ amplitude of the Fourier decomposition of the plasma boundary shape that is provided as input for the VMEC equilibrium calculation. The corresponding rotational transform ι profiles for the three cases under consideration are shown in Fig. 1c. We concentrate on the conditions that govern local ideal MHD properties in this paper. Resistive instabilities of the interchange and tearing mode type that can be of concern in the vicinity of the $\iota = 2/3$ and $2/4$ resonances are not addressed here.

We will specifically examine the relevant physical quantities described in the previous section on toroidal magnetic flux surfaces near midvolume at $s = 0.5612$ and near the edge of the plasma at $s = 0.949$. At $s = 0.5612$, the ballooning eigenvalues are $\lambda \simeq 0.2$, $\lambda \simeq 0.02$ and $\lambda \simeq -0.07$ for the vanishing, parabolic and hollow toroidal current cases, respectively. At $s = 0.949$, the corresponding ballooning eigenvalues are $\lambda = -0.55$, -1.6 and -0.12, respectively. Positive values denote instability and increasingly negative eigenvalues are associated with enhanced ballooning stability. Thus the hollow current profile yields the most stable conditions near midvolume but is the closest to marginality near the edge of the plasma. In more general terms for the pressure profile considered, the hollow current profile case is approximately optimal with respect to internal MHD modes as the ballooning calculations for the other two cases reveal instability in the inner two thirds of the plasma volume.

The most unstable ballooning eigenvalues occur on magnetic field lines that traverse the region where the normal curvature interaction with the pressure gradient attains its most negative value and the ballooning structures become correspondingly localised in that region. The distribution of $2p'(s)\sqrt{g}\boldsymbol{\kappa} \cdot \boldsymbol{\nabla} s$ on the surfaces at $s = 0.5612$ and $s = 0.949$ are displayed in Fig. 2 for the cases of hollow current profile, vanishing current and parabolic current profile. At $s = 0.5612$, the most negative values achieved for $2p'(s)\sqrt{g}\boldsymbol{\kappa} \cdot \boldsymbol{\nabla} s$ are approximately -2.9 for hollow

current, -3.2 for zero current and -2.7 for peaked current. At $s = 0.949$, the corresponding values are -2.4, -1.8 and -1.2, respectively. These results are basically in line with the relative magnitudes of the ballooning eigenvalues reported. The exception to the rule is the parabolic current case which has a larger ballooning eigenvalue despite a less destabilising magnitude of $2p'(s)\sqrt{g}\boldsymbol{\kappa} \cdot \boldsymbol{\nabla} s$ in comparison with the hollow current case at $s = 0.5612$. This discrepancy can be accounted for through the enhanced field line bending stabilisation contribution $k_\perp^2$ when the current profile is hollow. The values of $k_\perp^2$ on the most unstable field line are shown in Fig. 3 for $s = 0.5612$ and for $s = 0.949$.

The local magnetic shear $\sqrt{g}S$, the geodesic curvature κ_g and the quasiperiodic ballooning curvature κ_p are shown in Fig. 4 for the hollow toroidal current case near midvolume at $s = 0.5612$. The $\sqrt{g}S$ and κ_g distributions become nearly vanishing in the region where $2p'(s)\sqrt{g}\boldsymbol{\kappa} \cdot \boldsymbol{\nabla} s$ acquires its largest negative and thus most destabilising value. The relevance of the local magnetic shear with respect to ballooning stability has already been highlighted in a heliotron/torsatron device [14]. The κ_p reaches its most negative value roughly where the $\sqrt{g}S$ distribution develops a large negative stripe. The characteristic patterns of $\sqrt{g}S$, κ_g and κ_p do not change qualitatively with current, current profile or radial position. However, the sign of κ_g is seen to flip under some conditions, but this does not seem to affect the ballooning stability properties.

4 CONCLUSION AND DISCUSSION

We have investigated the impact of a toroidal current and its profile on the driving and stabilising mechanisms for ballooning instabilities in a 2 period quasiaxisymmetric stellarator. We have found that the interaction of the pressure gradient with the normal curvature, as expected, plays a fundamental role in the description of ballooning stability properties. Ballooning modes localise where $2p'(s)\sqrt{g}\boldsymbol{\kappa} \cdot \boldsymbol{\nabla} s$ becomes large and negative. The local magnetic shear displays a helical stripe but is broadly vanishing where the normal curvature concentrates the ballooning structures. Although a hollow finite bootstrap current can enhance the susceptibility to global external kink mode destabilisation, the finite helical stripe in $\sqrt{g}S$ constitutes an important stabilising element for this type of structure. This issue will be addressed in detail in future work to be published. The quasiperiodic ballooning curvature κ_p develops a dominant contribution in the region where the local magnetic shear is large and thus represents an unreliable indicator of where ballooning structures peak. The geodesic curvature vanishes where $2p'(s)\sqrt{g}\boldsymbol{\kappa} \cdot \boldsymbol{\nabla} s$ is large and negative. Its spectrum is dominated by a $m/n = 1/0$ component and the amplitude of this modulation along a magnetic field line impacts the width of the ballooning eigenstructure. Near midvolume, the amplitude is largest for the hollow current profile case and is very small for zero current. Near the edge of the plasma,

the modulation amplitude of κ_g is weakest for the hollow current case and largest for vanishing current.

Near the edge of the plasma, a hollow toroidal current profile enhances the normal curvature while a parabolic current profile diminishes it compared with the vanishing current benchmark. This is reflected in the magnitude of the corresponding ballooning eigenvalues. Near midvolume, finite toroidal current reduces the normal curvature and the corresponding eigenvalues are less unstable. Though the normal curvatures with finite current are comparable at midvolume, the hollow current case is more resilient to ballooning mode destabilisation than the parabolic current profile case because the field line bending stabilisation is larger. The zero current case displays the largest field line bending contribution, but it is insufficient to compensate for the more adverse normal curvature.

Acknowledgments
This research was partially sponsored by the Fonds National Suisse de la Recherche Scientifique. One of the authors (WAC) would like to acknowledge the hospitality at NIFS during a stay as Invited Professor and the assistance of Professor K. Watanabe to install the codes required for this work on the local computer system. We thank Dr. S.P. Hirshman for use of the VMEC equilibrium code.

References

[1] BOOZER, A.H., 1980 Phys. Fluids **23** 904.

[2] NÜHRENBERG, J., LOTZ, W., GORI, S., 1994 *Quasi-axisymmetric Tokamaks*, in Proc. Joint Varenna-Lausanne Int. Workshop on Theory of Fusion Plasmas, Editrice Compositori, Bologna 3.

[3] GARABEDIAN, P.R., 1996 Phys. Plasmas **3** 2483.

[4] OKAMURA, S., MATSUOKA, K., FUJIWARA, M., DREVLAK, M., MERKEL, P., NÜHRENBERG, J., 1998 J. Plasma Fusion Res. **1** 164.

[5] NEILSON, G.H., REIMAN, A.H., ZARNSTORFF, M.C., BROOKS, A., FU, G.Y., GOLDSTON, R.J., KU, L.P., LIN, Z., MAJESKI, R, MONTICELLO, D.A., MYNICK, H., POMPHREY, N., REDI, M.H., REIERSEN W.T., SCHMIDT J.A., HIRSHMAN, S.P., LYON, J.F., BERRY, L.A., NELSON, B.E., SANCHEZ, R., SPONG, D.A., BOOZER, A.H., MINER, W.H., VALANJU, P.M., COOPER, W.A., DREVLAK, M., MERKEL, P., NÜHRENBERG, C., 2000 Phys. Plasmas **7** 1911.

[6] CORREA-RESTREPO, D., 1978 Z. Naturforsch. **33a** 789.

[7] CONNOR, J.W., HASTIE, R.J., TAYLOR, J.B, 1979 Proc. R. Soc. London Ser. A **365** 1.

[8] DEWAR, R.L., GLASSER, A.H., 1983 Phys. Fluids **26** 3038.

[9] GREENE, J.M., JOHNSON, J.L., 1968 Plasma Phys. **10** 729.

[10] GREENE, J.M., CHANCE, M.S., 1981 Nucl. Fusion **21** 453.

[11] COOPER, W.A., 1997 Phys. Plasmas **4** 153.

[12] HEGNA, C.C., NAKAJIMA, N., 1998 Phys. Plasmas **5** 1336.

[13] HIRSHMAN, S.P., BETANCOURT, O., 1991 J. Comput. Phys. **96** 99.

[14] NAKAJIMA, N., 1996 Phys. Plasmas **3** 4556.

Figures

FIG. 1. (a) The pressure profile prescribed (top), (b) the toroidal plasma current profiles prescribed (middle) and (c) the rotational transform profiles in a 2 period quasiaxisymmetric stellarator at $\beta^* \simeq 3\%$ for a parabolic current profile, a hollow current profile and vanishing current (bottom). The normalised current is $2\pi J_N = 0.2552$. The locations of the critical resonant surfaces $\iota = 1/2$ and $\iota = 2/3$ are identified.

FIG. 2. The distributions of the interaction of the normal curvature with the pressure gradient $2p'(s)\sqrt{g}\boldsymbol{\kappa} \cdot \boldsymbol{\nabla} s$ for the hollow toroidal current profile case (top), the vanishing current case (middle) and the parabolic toroidal current case (bottom) near midvolume at $s = 0.5612$ (left) and near the edge of the plasma at $s = 0.949$ (right) for a 2 period quasiaxisymmetric stellarator at $\beta^* \simeq 3\%$.

FIG. 3. The field line bending term $k_\perp^2$ on the most ballooning unstable field line near midvolume at $s = 0.5612$ (top) and near the edge of the plasma at $s = 0.949$ (bottom) for vanishing current, hollow toroidal current and parabolic toroidal current in a 2 period quasiaxisymmetric stellarator at $\beta^* \simeq 3\%$. For finite current, the normalised current is $2\pi J_N = 0.2552$.

FIG. 4. The distributions of the local magnetic shear $\sqrt{g}S$ (top), the geodesic curvature κ_g (middle) and the quasiperiodic ballooning curvature (bottom) in a quasiaxisymmetric stellarator with hollow toroidal current profile at $\beta^* \simeq 3\%$ on a flux surface near midvolume at $s = 0.5612$.

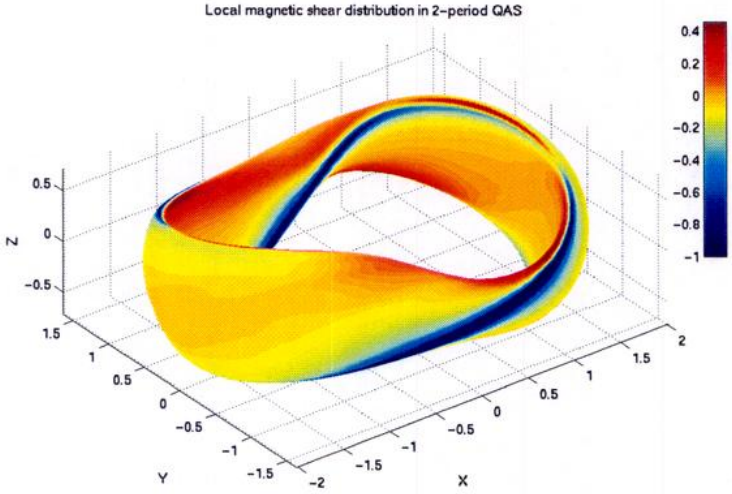
Local magnetic shear distribution in 2-period QAS
0.4
0.2
0
−0.2
−0.4
−0.6
−0.8
−1
Z
0.5
0
−0.5
Y
1.5
1
0.5
0
−0.5
−1
−1.5
X
−2
−1.5
−1
−0.5
0
0.5
1
1.5
2

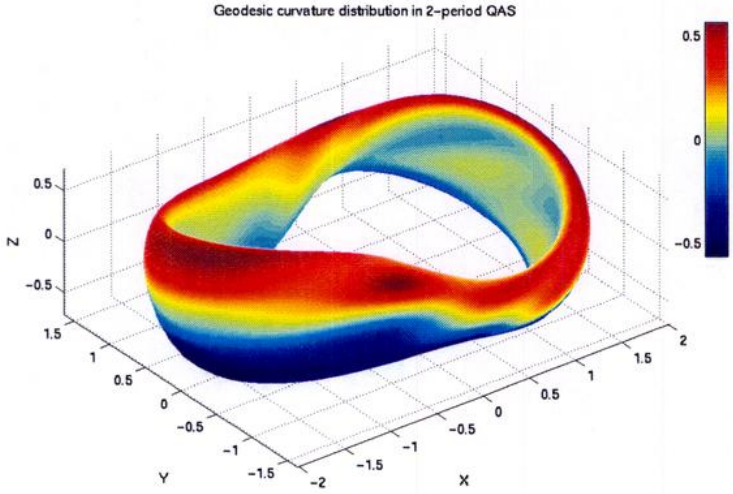
Geodesic curvature distribution in 2-period QAS
0.5
0
−0.5
Z
0.5
0
−0.5
Y
1.5
1
0.5
0
−0.5
−1
−1.5
X
−2
−1.5
−1
−0.5
0
0.5
1
1.5
2

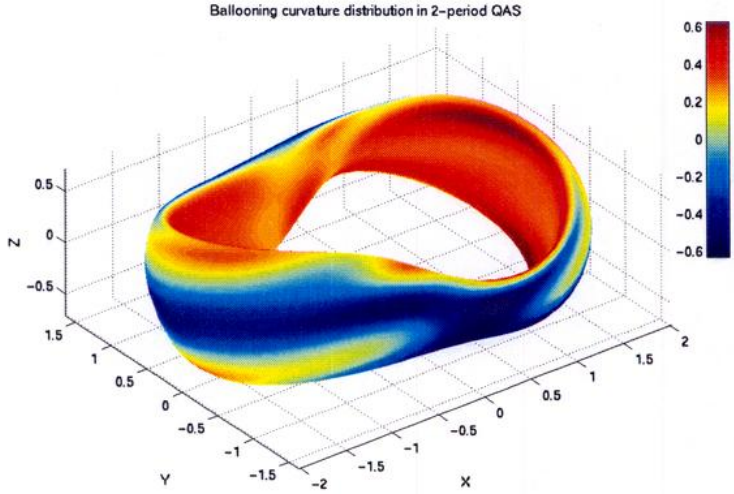
Ballooning curvature distribution in 2-period QAS
0.6
0.4
0.2
0
−0.2
−0.4
−0.6
Z
0.5
0
−0.5
Y
1.5
1
0.5
0
−0.5
−1
−1.5
X
−2
−1.5
−1
−0.5
0
0.5
1
1.5
2

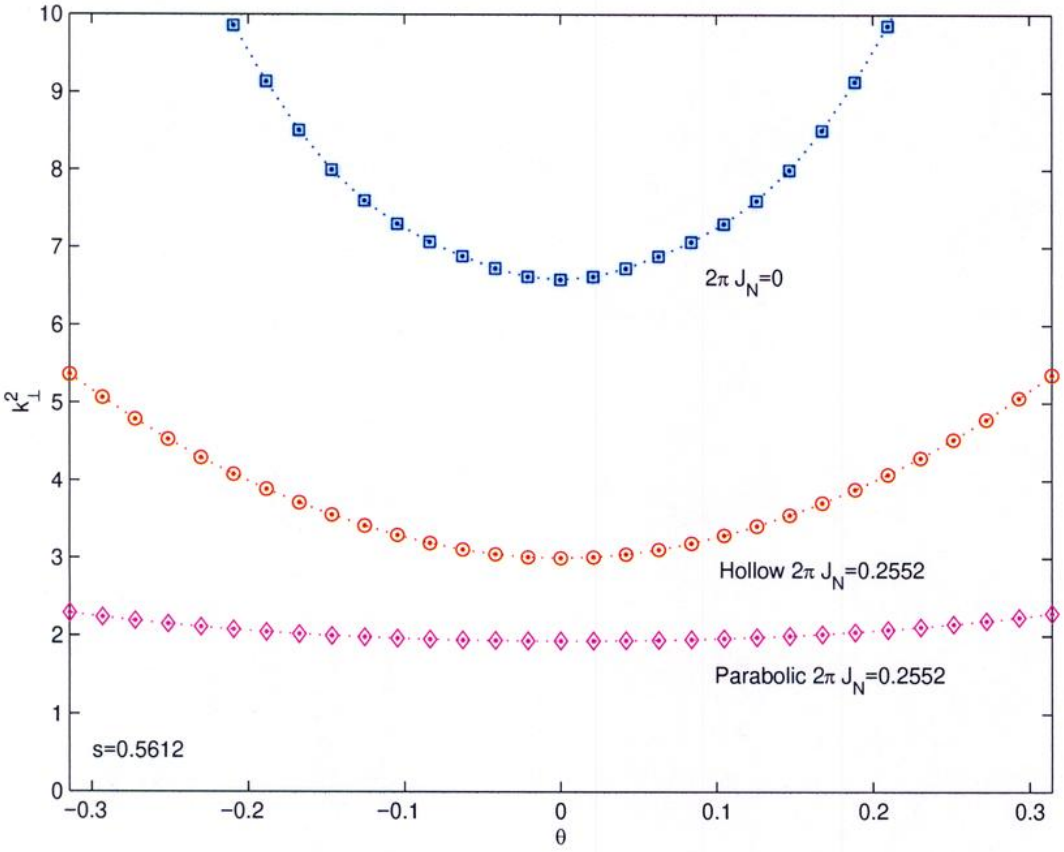
$2\pi J_N=0$
Hollow $2\pi J_N=0.2552$
Parabolic $2\pi J_N=0.2552$
s=0.5612
$k_\perp^2$
θ

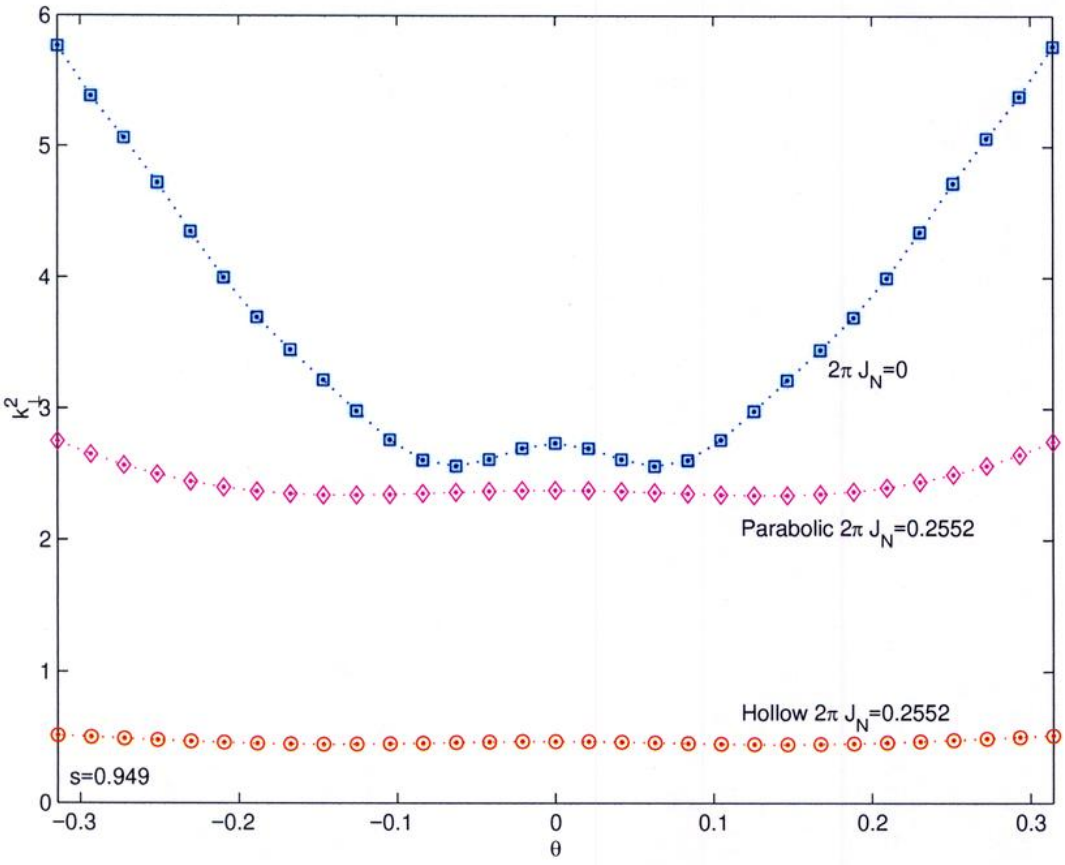
$2\pi J_N=0$
Parabolic $2\pi J_N=0.2552$
Hollow $2\pi J_N=0.2552$
s=0.949
$k_\perp^2$
θ

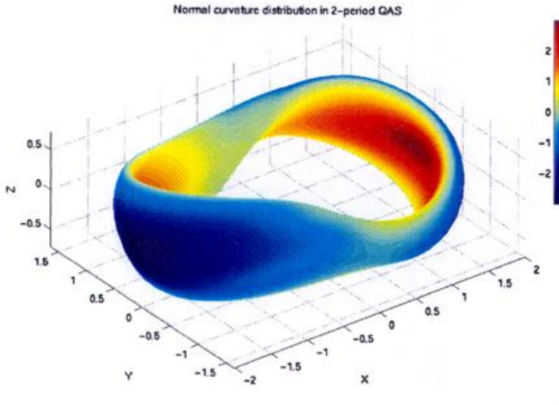
Normal curvature distribution in 2-period QAS
Z
Y
X

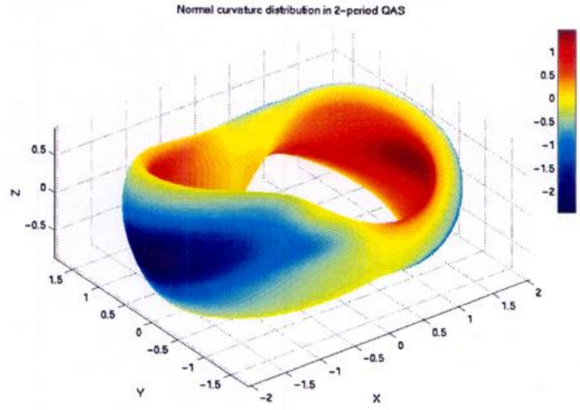
Normal curvature distribution in 2-period QAS
Z
Y
X

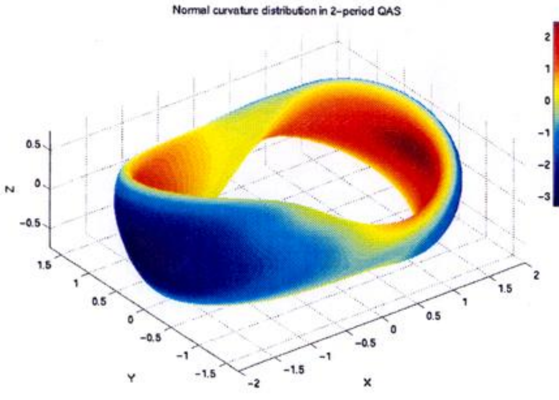
Normal curvature distribution in 2-period QAS
Z
Y
X

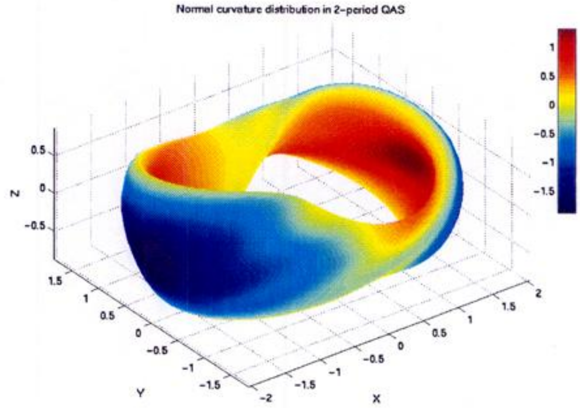
Normal curvature distribution in 2-period QAS
Z
Y
X

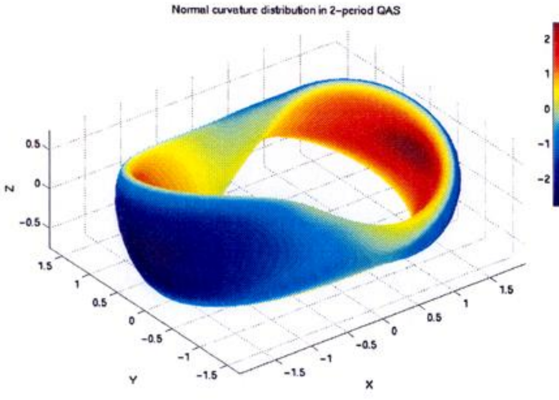
Normal curvature distribution in 2-period QAS
Z
Y
X

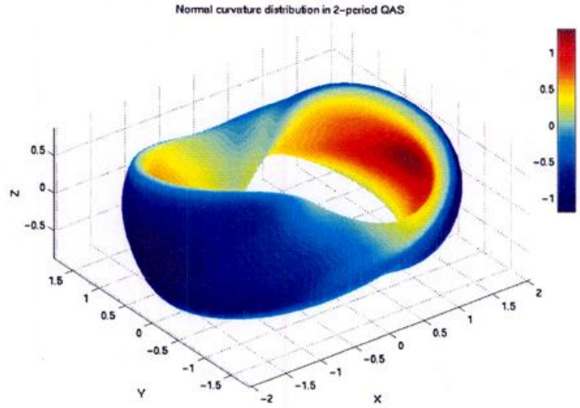
Normal curvature distribution in 2-period QAS
Z
Y
X

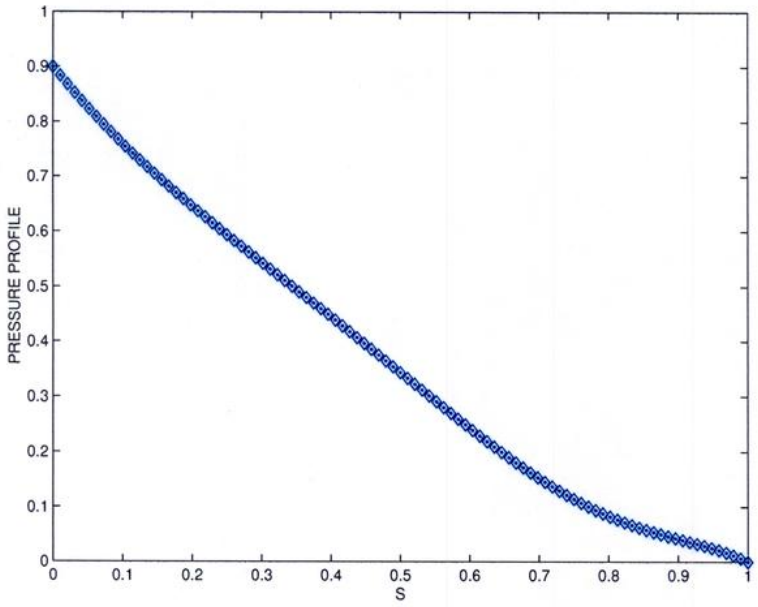
PRESSURE PROFILE
S

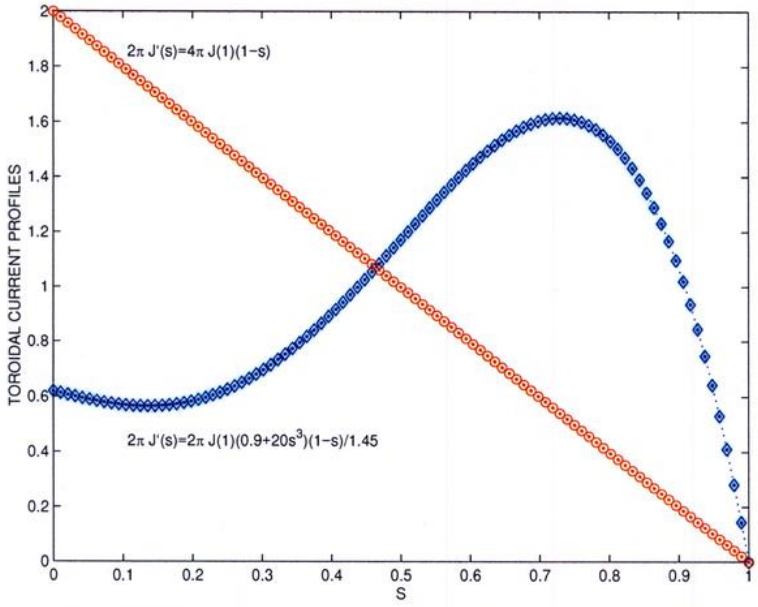
2π J'(s)=4π J(1)(1−s)
2π J'(s)=2π J(1)(0.9+20s^3)(1−s)/1.45
TOROIDAL CURRENT PROFILES
S

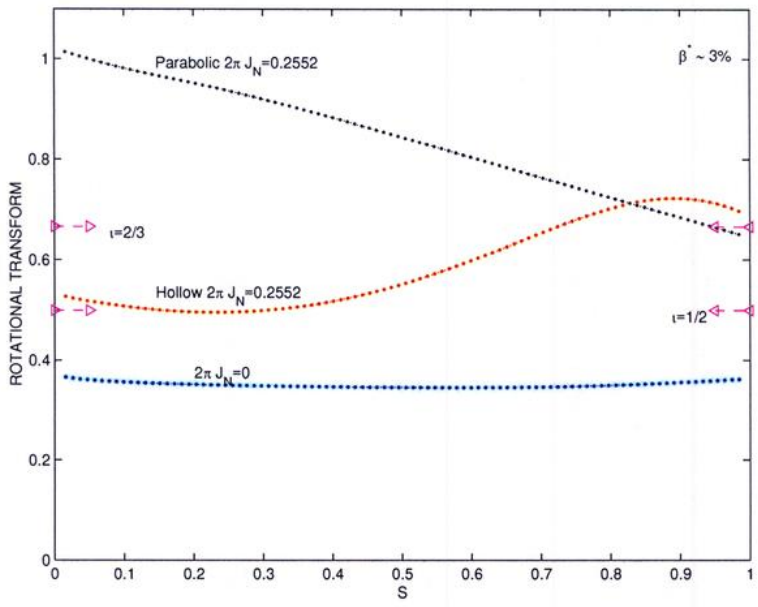
Parabolic 2π J_N=0.2552
β* ~ 3%
ι=2/3
Hollow 2π J_N=0.2552
ι=1/2
2π J_N=0
ROTATIONAL TRANSFORM
S